

Negative thermal expansion in NbF_3 and $NbOF_2$: A comparative theoretical study

Mingyue Zhang(张明月), Chunyan Wang(王春艳), Yinuo Zhang(张一诺), Qilong Gao(高其龙), Yu Jia(贾瑜)

Citation: Chin. Phys. B, 2021, 30 (**5**): 056501. DOI: 10.1088/1674-1056/abe376
Journal homepage: http://cpb.iphy.ac.cn; http://iopscience.iop.org/cpb

What follows is a list of articles you may be interested in

Negative thermal expansion of Ca_2RuO_4 with oxygen vacancies

Sen Xu(徐森), Yangming Hu(胡杨明), Yuan Liang(梁源), Chenfei Shi(史晨飞), Yuling Su(苏玉玲), Juan Guo(郭娟), Qilong Gao(高其龙), Mingju Chao(晁明举), Erjun Liang(梁二军)

Chin. Phys. B, 2020, 29 (**8**): 086501. DOI: 10.1088/1674-1056/ab8a36

Properties of negative thermal expansion *β*-eucryptite ceramics prepared by spark plasma sintering

Li-Min Zhao(赵利敏), Yong-Guang Cheng(程永光), Hao-Shan Hao(郝好山), Jiao Wang(王娇), Shao-Hui Liu(刘少辉), Bao-Sen Zhang(张宝森)

Chin. Phys. B, 2018, 27 (**9**): 096501. DOI: 10.1088/1674-1056/27/9/096501

Negative thermal expansion and photoluminescence in solid solution $(HfSc)_{0.83}W_{2.25}P_{0.83}O_{12\delta}$

Yuan Liang(梁源), Yong-Guang Cheng(程永光), Xiang-Hong Ge(葛向红), Bao-He Yuan(袁保合), Juan Guo(郭娟), Qian Sun(孙强), Er-Jun Liang(梁二军)

Chin. Phys. B, 2017, 26 (**10**): 106501. DOI: 10.1088/1674-1056/26/10/106501

Anomalous low-temperature heat capacity in antiperovskite compounds

Xin-Ge Guo(郭新格), Jian-Chao Lin(林建超), Peng Tong(童鹏), Shuai Lin(蔺帅), Cheng Yang(杨骋), Wen-Jian Lu(鲁文建), Wen-Hai Song(宋文海), Yu-Ping Sun(孙玉平)

Chin. Phys. B, 2017, 26 (**2**): 026501. DOI: 10.1088/1674-1056/26/2/026501

Zero and controllable thermal expansion in $HfMgMo_{3-x}W_xO_{12}$

Tao Li(李涛), Xian-Sheng Liu(刘献省), Yong-Guang Cheng(程永光), Xiang-Hong Ge(葛向红), Meng-Di Zhang(张孟迪), Hong Lian(连虹), Ying Zhang(张莹), Er-Jun Liang(梁二军), Yu-Xiao Li(李玉晓)

Chin. Phys. B, 2017, 26 (**1**): 016501. DOI: 10.1088/1674-1056/26/1/016501

Negative thermal expansion in NbF_3 and $NbOF_2$: A comparative theoretical study*

Mingyue Zhang(张明月)[1], Chunyan Wang(王春艳)[1,2], Yinuo Zhang(张一诺)[1], Qilong Gao(高其龙)[1,†], and Yu Jia(贾瑜)[2,1,‡]

[1] International Laboratory for Quantum Functional Materials of Henan, and School of Physics and Microelectronics, Zhengzhou University, Zhengzhou 450052, China

[2] Key Laboratory of Special Functional Materials of Ministry of Education, and School of Materials Science and Engineering, Henan University, Henan 475001, China

(Received 20 December 2020; revised manuscript received 1 February 2021; accepted manuscript online 5 February 2021)

Thermal expansion control is always an obstructive factor and challenging in high precision engineering field. Here, the negative thermal expansion of NbF_3 and $NbOF_2$ was predicted by first-principles calculation with density functional theory and the quasi-harmonic approximation (QHA). We studied the total charge density, thermal vibration, and lattice dynamic to investigate the thermal expansion mechanism. We found that the presence of O induced the relatively strong covalent bond in $NbOF_2$, thus weakening the transverse vibration of F and O in $NbOF_2$, compared with the case of NbF_3. In this study, we proposed a way to tailor negative thermal expansion of metal fluorides by introducing the oxygen atoms. The present work not only predicts two NTE compounds, but also provides an insight on thermal expansion control by designing chemical bond type.

Keywords: negative thermal expansion, fluorides, lattice dynamics calculation, average atomic volume, negative Grüneisen parameters

PACS: 65.40.De, 61.66.–f, 71.30.+h, 61.72.Jd **DOI:** 10.1088/1674-1056/abe376

1. Introduction

Negative thermal expansion (NTE) is an interesting physical phenomenon, in which volume shrinks rather than expands with increasing temperature.[1–3] The presence of NTE materials offers a promising possibility to control the thermal expansion in optical, electronic, and engineering applications.[4] So far, a number of families of NTE materials have been identified such as alloy,[5] oxides,[6–9] fluorides,[10,11] cyanides,[12,13] Prussian blue analogues (PBAs),[14,15] metal-organic frameworks,[16,17] manganese nitrogen compounds,[18,19] and so on. However, compared with the number of positive thermal expansion (PTE) materials, the quantity and variety of NTE materials are very small, thus limiting their further applications. Hence, nowadays, exploring or predicting new NTE materials and further understanding NTE mechanism are always urgent and challenging.

Due to the presence of the unique ionic bond character, the NTE behavior has been found in some ReO_3-type metal fluorides. For example, the simplest cubic structure of ScF_3 with the wide-temperature-window (10–1100 K) and large isotropic NTE (60–110 K, $\alpha_l \approx -14$ ppm·K^{-1}) has been reported by experiment in 2010. It is the only one found in single ReO_3-type metal fluorides. The double-ReO_3-type, such as $CaZrF_6$ and $CaHfF_6$ were found with much larger isotropic NTE ($\alpha_l \approx -18$ ppm·K^{-1} and -20 ppm·K^{-1} at 100 K) than that of ScF_3.[11] Then based on the chemical general formula $A^{II}B^{IV}F_6$, several NTE materials were found, such as $CaNbF_6$,[20] $MnZrF_6$,[21] and $CaTiF_6$.[22] However, the NTE fluoride materials have also very litter. For the thermal expansion control, it always adopts the chemical modification in cations. For example, chemical substitution in $(Sc_{1-x}M_x)F_3$ (M = Al, Ti, Fe and Ga)[22–25] or by redox intercalation in $Li_x(Sc_{0.9}Fe_{0.1})F_3$,[26] the crossover from NTE to zero thermal expansion (ZTE) and finally to PTE was widely observed. It also has been observed that it could been adjusted by the F-excess such as $TiZrF_{7-x}$[7] and $Mg_{1-x}Zr_{1+x}F_{6+2x}$.[28] Recently, we notice that the NbF_3 has the cubic ReO_3 type crystal structure, which represents a typical structure of $TMO_{3-x}F_x$ (TM = Nb, Ta, Ti, Mo, and W).[29,30] Similar thermal expansion control behavior occurs in many oxides materials such as NH_3 in ZrW_2O_8[31] and $Zr_{0.5}Hf_{0.5}VPO_7$.[32] More recently, Li *et al.*[33] reported that the chemical bond had larger effect on the NTE behavior in $MCo(CN)_6$ (M = Fe, Ti, Co). It naturally leads us to assume that if we adjust part chemical bond in NbF_3, the NTE behavior maybe have some change. It is an interesting idea to tailor negative NTE by designing the chemical bond.

In this work, the NTE, electronic structure, lattice dynam-

*Project supported by the National Natural Science Foundation of China (Grant Nos. 11774078 and 21905252), China Postdoctoral Science Foundation (Grant No. 2019M652558), and Innovation Scientists and Technicians Troop Construction Projects of Henan Province, China (Grant No. 10094100510025).

†Corresponding author. E-mail: qilonggao@zzu.edu.cn

‡Corresponding author. E-mail: jiayu@henu.edu.cn

© 2021 Chinese Physical Society and IOP Publishing Ltd

ics of NbF_3 and $NbOF_2$ are investigated by first-principles calculations with density functional theory and the quasi-harmonic approximation. We show that the NTE of $NbOF_2$ is smaller than that of NbF_3 and the driving force of NTE in $NbOF_2$ comes from the transverse vibration of the F and O atoms, while the vibration amplitude of the O atoms is much smaller than that of the F atoms.

2. Computational details

All the results are calculated using density functional theory (DFT) as implemented in the Vienna *ab into* simulation package (VASP) code.[34] The ion–electron interaction is depicted by projector augmented wave (PAW) method[35] and the exchange and correlation effects are described by the generalized gradient approximation with PBE functional.[36] The energy cutoff is 520 eV and an $11\times11\times11$ k-points mesh has been used to obtain the total energy convergence. The convergence criteria for the total energy and ionic forces are set to 10^{-8} eV and 10^{-3} eV/Å, respectively.

Phonon disoersion spectra of NbF_3 and $NbOF_2$ are calculated by frozen phonon method within a $2\times2\times2$ supercell and post processed by PHONOPY code.[37] A $2\times2\times2$ grid is used for the Brillouin-zone integration. The thermodynamic properties are simulated through the quasi-harmonic approximation (QHA) theory. In this approximation, the volume dependent phonon frequencies at finite temperatures are introduced as a part of the anharmonic effect. In our previous works, this method provided reasonable and interesting description of the dynamic properties of materials below the melting point.[38–41] Within the QHA, the phonon contribution to the Helmholtz free energy $F(V,T)$ can be written as

$$F(V,T) = E(V) + F_{\mathrm{vib}}(V,T), \tag{1}$$

where $E(V)$ is the total static energy form DFT calculations, $F_{\mathrm{vib}}(V,T)$ stands for the vibration energy and is calculated by

$$F_{\mathrm{vib}}(V,T) = k_{\mathrm{B}}T\sum_{v,q}\log\left\{2\sinh\left(\frac{\hbar\omega v(q,v)}{2k_{\mathrm{B}}T}\right)\right\}, \tag{2}$$

where $\omega v(q,v)$ is the phonon frequency at a fixed volume V and a given vector q. In order to obtain the effect of temperature on volume, 11 diffferent volumes are selected near the optimized equilibrium position.

3. Results and discussion

3.1. Crystal structures and coefficient of thermal expansion

As mentioned in the introduction, NbF_3 and $NbOF_2$ crystallize in cubic structure with the space group (Pm-3m), and the unit cell contains one formula unit with 4 atoms.[29,42] Nb and O(F) atoms lie at 1a(0, 0, 0) and 3d(0.5, 0, 0) Wyckoff sites, respectively. The crystal structure is composed of NbF_6 or NbO_6 octahedra, which is isostructural with ScF_3, as shown in Figs. 1(a) and 1(b). In our calculation, the lattice constants of NbF_3 and $NbOF_2$ are 4.11860 Å and 4.10951 Å, respectively. The temperature dependence of the cell volume and the coefficients of thermal expansion (CTE) of NbF_3 and $NbOF_2$ are present in Figs. 1(c) and 1(d), respectively. It is found that the cell volumes at a finite temperature for both NbF_3 and $NbOF_2$ are smaller than those at 0 K, exhibiting a typical NTE behavior. The largest CTE for NbF_3 is about -31×10^{-6} K^{-1} at 100 K, while for $NbOF_2$, the largest CTE is about -9×10^{-6} K^{-1}. Hence, this implies that the NTE behavior could be tailored by the introduction of O atom in NbF_3. More importantly, the underlying mechanism of such large differences between them in NTE should be noticed and need to study.

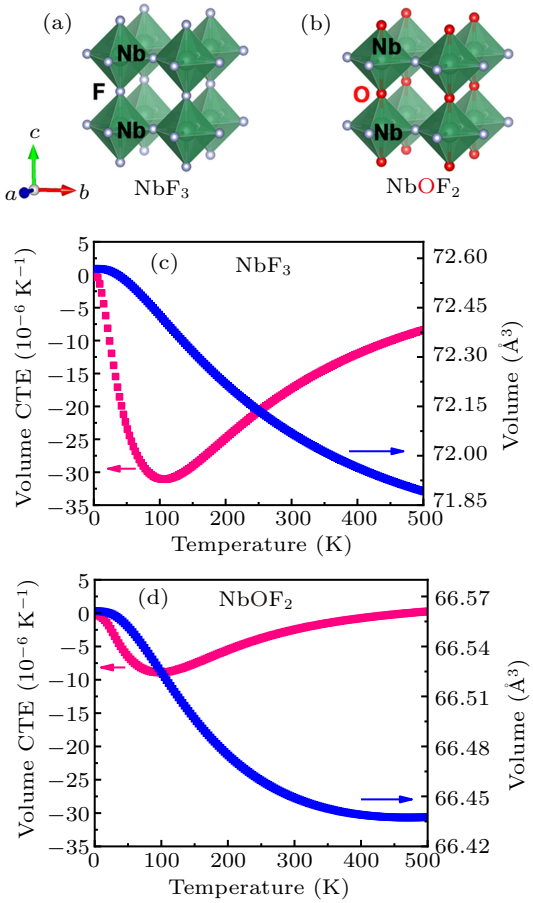


Fig. 1. (a), (b) Geometric structures of NbF_3 and $NbOF_3$, (c), (d) temperature dependence of the cell volume and CNTE of NbF_3 and $NbOF_2$, respectively.

3.2. Negative thermal expansion mechanism and role of O atoms in $NbOF_2$

In order to investigate the underlying mechanism responsible for the NTE of NbF_3 and the role of O atoms in $NbOF_2$, we have calculated the corresponding phonon spectrum, partial phonon density of states (DOS), and Grüneisen parameters

of NbF_3 and $NbOF_2$ compounds, as shown in Figs. 2(a) and 2(b). It is shown that the phonon dispersion curves along the high-symmetry lines of the Brillouin zone (BZ) have no imaginary frequencies, indicating that NbF_3 and $NbOF_2$ are dynamically stable. In the region of high frequency, it is the vibration of F atoms for NbF_3 while for $NbOF_2$, it is the vibration of O atoms. In the region of low frequency, compared with NbF_3, the substitution of O makes the frequencies at M and R points increase, and the frequency at M point is higher than that at R point. As shown in DOS (Figs. 2(a) and 2(b) right), the contribution to vibrational frequency below 200 cm^{-1} is mainly from F atoms. However, the vibration of F atoms is suppressed in $NbOF_2$, which suggests that the vibrations associated with F atoms are easy to be excited predominantly at low temperatures for NbF_3, while it is inhibited in $NbOF_2$. Figures 2(c) and 2(d) display the calculated Grüneisen parameters as a function of vibrational frequency in Brillouin zone (inset along high symmetry directions). In general, the Grüneisen parameter reflects the anharmonic effect, i.e., the nonlinear vibrational modes of atoms.[43] If the sum of negative Grüneisen parameters (γ_i) for the excited modes is larger than that of the positive ones, the CTE of the material will be negative.[43] Similar to ScF_3, obviously, the M(0.5 0.5 0) and R(0.5 0.5 0.5) points at Brillouin-zone boundary have the largest negative values.[44] The corresponding negative Grüneisen parameters of $NbOF_2$ are much smaller than those of NbF_3, thus introducing a smaller CTE.

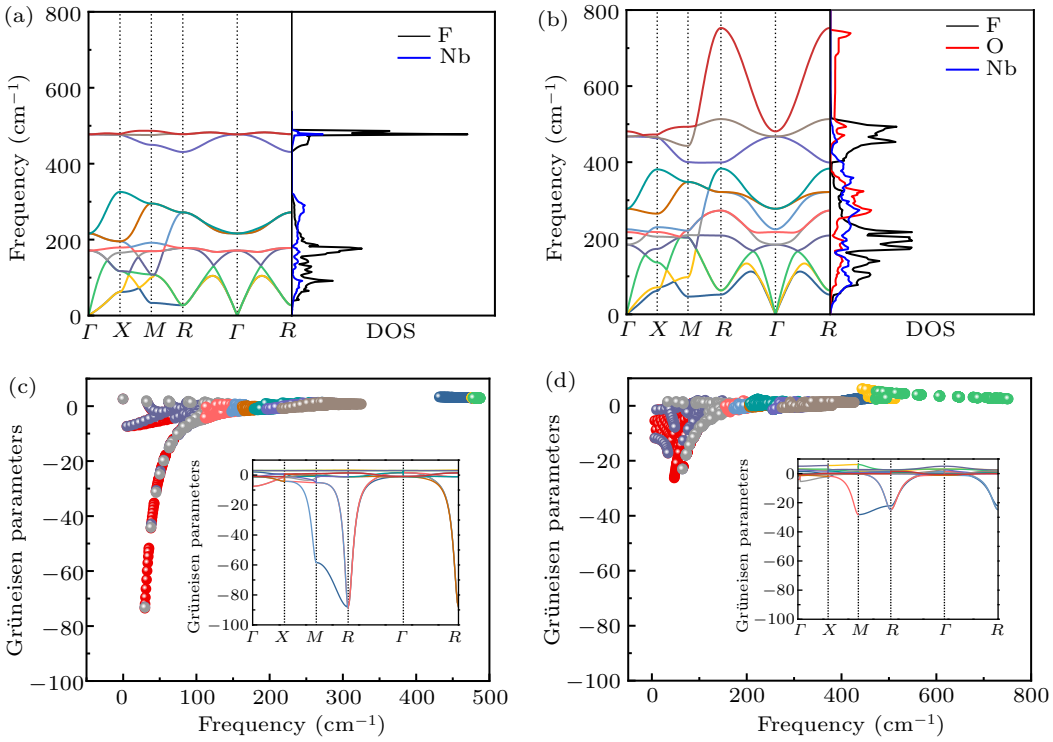


Fig. 2. (a), (b) Calculated phonon dispersion curves and partial density of states (DOS). (c), (d) Calculated Grüneisen parameters as a function of vibrational frequency (inset along high symmetry directions) for NbF_3 and $NbOF_2$, respectively.

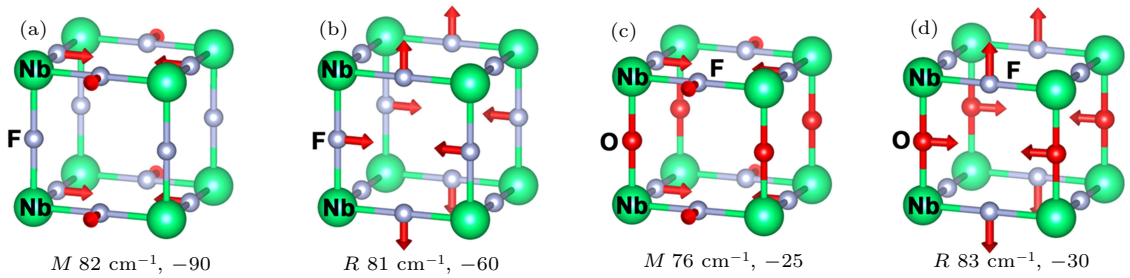


Fig. 3. Atomic displacement schemes for low frequency vibrational modes at M and R points. (a), (c) NbF_3 and (b), (d) $NbOF_2$.

Since the NTE is closely related to the modes with relative large negative Grüneisen parameters, we have therefore studied these vibrations modes to further shed light on the mechanism. The low-energy vibrational modes of NbF_3 and $NbOF_2$ at M and R points are shown in Fig. 3. At M point, for NbF_3, F atoms have transverse vibrations in the *ab*-plane and the metal Nb atoms are stock-still, resulting in a librational motion of undistorted NbF_6 octahedra. The coupling rotations of the adjacent octahedra shorten the effective length of neighboring metal–metal atoms, therefore contributing to

the NTE behavior. For the $NbOF_2$, as well as NbF_3, it is the transverse vibrations of F atoms in the *ab*-plane that contribute to the NTE. At *R* points, for NbF_3, it is the vibration mode of triple merger along three sides. For $NbOF_3$, it is not the same three vibration modes, so the merger is broken up. It should be noted that at the metal–O (or F)–metal linkage, the amplitude of vibration of O atoms is smaller than that of F atom.

On the other hand, the strength of chemical bonding has great impact on the NTE behavior of framework compounds.[33] To further illustrate the relationship between chemical bonding and NTE phenomenon, the charge densities on (010) plane are shown in Figs. 4(a) and 4(b) for NbF_3 and $NbOF_2$, respectively. We can see an obvious ionic bonding character between Nb and F, while in $NbOF_2$, an evident covalent character between Nb and O, and an ionic bonding character between Nb and F. Hence, the bond of Nb–O is much stiffer than the Nb–F bond, so the transverse vibration of O atoms is more difficult than that of F, and hence the $NbOF_2$ system exhibits a small NTE behavior.

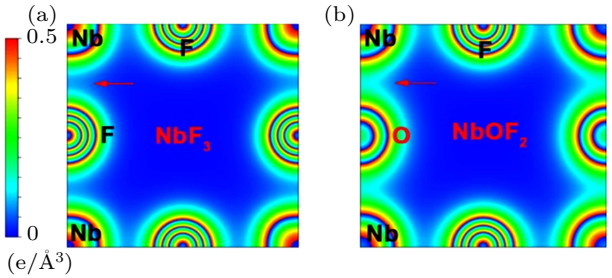


Fig. 4. Charge densities of NbF_3 (a) and $NbOF_2$ (b) on (010) plane.

3.3. Average atomic volume and atomic displacement parameters

It should be noted that the NbF_3 and $NbOF_2$ have an open-framework structure. The NTE behavior of open-framework compounds has strong relationship with the structure flexibility.[2,15] Recently, we noted the concept of average atomic volume (AAV) to explore new NTE materials.[45] Interesting, the AAV of NbF_3 is about 18 Å^3 at 300 K, which is much larger than the critical AAV ($\sim$ 16 Å^3). While the AAV of $NbOF_2$ is about 16.6 Å^3, which is also larger the critical AAV but samller than that of NbF_3. Hence, the reduction of AAV should be a key factor for the difference of NTE behavior by the introduction of O atoms. The anisotropic atomic displacement parameters (ADPs) also could quantify the effect of the induction of O atoms in NbF_3 and $NbOF_2$. Like most of open-framework NTE compounds, the NTE comes from the transverse thermal vibration of bridge atoms.[10,12,46] Obviously, the transverse vibration of F atoms in NbF_3 and $NbOF_2$ is almost the same, while larger than that of O atoms (Fig. 2). Hence, the introduction of O atoms weakens the transverse vibration of bridge atoms, thus producing the inhibiting effect. The energy barrier versus non-metal atoms displace is investigated to reflect the transverse vibration potential of bridge atoms.[47] The energy potential curves of F atoms in NbF_3 and both F and O atoms in $NbOF_2$ are obtained by changing the atom position along the vibrating direction, as shown in Fig. 5(a).

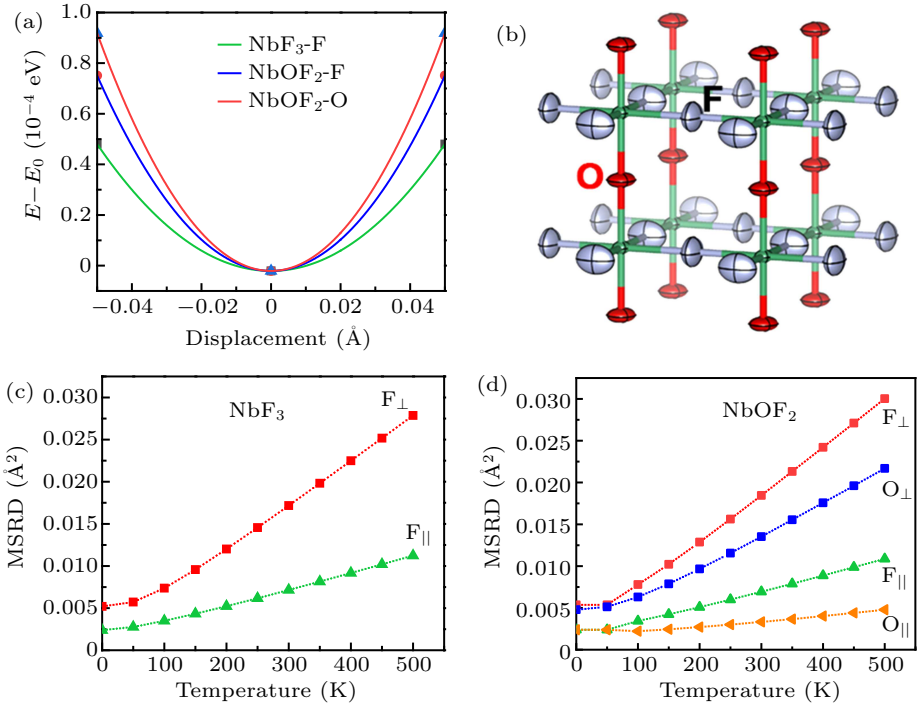


Fig. 5. (a) Energy difference versus non-metal atoms displace. (b) The anisotropic displacement ellipsoids at 300 K, the atoms are represented as ellipsoids that reflect the distribution of thermal displacements. The distributions of displacements of the anions are strongly elongated in the transverse directions perpendicular and parallel to the bond for (c) NbF_3 and (d) $NbOF_2$, respectively.

Obviously, the energy difference in $NbOF_2$ is steeper than that in NbF_3, which indicate that the corresponding atomic vibration in $NbOF_2$ is more difficult than that in NbF_3. In all, considering that there is no obvious difference of lattice constants between NbF_3 and $NbOF_2$ from our calculation, we conclude that, if we introduce the O atom to NbF_3, the CTE of NTE in NbO_xF_{3-x} can be easily tuned from -9×10^{-6} K^{-1} to -30×10^{-6} K^{-1} without the structures distorted. This provides an ideal NTE material for realizing composite material with zero thermal expansion.

4. Conclusion

In summary, the NTE behavior and mechanism of cubic NbF_3 and $NbOF_2$ are investigated by using first-principles calculations within density functional theory and the quasi-harmonic approximation. NbF_3 shows strong NTE due to the transverse vibration modes of F atoms, once the 1/3 F atoms are substituted by O atoms, the transverse vibration of the F atoms is hindered, thus the NTE will be reduced. Combined with the eigenvectors of phonon modes corresponding to the NTE behavior, electronic properties, and total-energy of atoms-displaced configurations, the NTE of NbF_3 is larger than that of $NbOF_2$ due to the produce of covalent chemical bond by O atoms. The present work not only predicts two new NTE compounds, but also provides an insight on thermal expansion control.

Acknowledgment

Zhang Mingyue thanks Dr. Li Chong for his technical support.

References

[1] Mary T A, Evans J S O, Vogt T and Sleight A 1996 *Science* **272** 90
[2] Chang D, Niu C Y, Huang X, Sun Q, Cho J H and Jia Y 2017 *Phys. Rev. B* **95** 104101
[3] Mittal R, Gupta M K and Chaplot S L 2018 *Prog. Mater. Sci* **92** 360
[4] Chen J, Hu L, Deng J X and Xing X R 2015 *Chem. Soc. Rev* **44** 3522
[5] Song Y Z, Chen J, Liu X Z, Wang C W, Zhang J, Liu H, Zhu H, Hu L, Lin K, Zhang S T and Xing X R 2018 *J. Am. Chem. Soc* **140** 602
[6] Liu F S, Chen X P, Xie H X, Ao W Q and Li J Q 2010 *Acta. Phys. Sin.* **59** 3350 (in Chinese)
[7] Xu S, Hu Y, Liang Y, Shi C, Su Y, Guo J, Gao Q L, Chao M and Liang E J 2020 *Chin. Phys. B* **29** 086501
[8] Sanson A 2014 *Chem. Mater.* **26** 3716
[9] Ge X H, Mao Y C, Li L, Li L P, Yuan N, Cheng Y G, Guo J, Chao M J and Liang E J 2016 *Chin. Phys. Lett* **33** 046503
[10] Greve B K, Martin K L, Lee P L, Chupas P J, Chapman K W and Wilkinson A P 2010 *J. Am. Chem. Soc.* **132** 15496
[11] Hancock J C, Chapman K W, Halder G J, Morelock C R, Kaplan B S, Gallington L C, Bongiorno A, Chu H, Si Z and Wilkinson A P J C 2015 *Chem. Mater.* **27** 3912
[12] Hibble S J, Chippindale A M, Marelli E, Kroeker S, Michaelis V K, Greer B J, Aguiar P M, Bilbe E J, Barney E R and Hannon A C 2013 *J. Am. Chem. Soc.* **135** 16478
[13] Gao Q L, Liang E J, Xing X R and Chen J 2020 *Chem. J. Chin. U.* **41** 388
[14] Li M, Li Y, Wang C Y and Sun Q 2019 *Chin. Phys. Lett.* **36** 066301
[15] Gao Q L, Sun Y, Shi N K, Milazzo R, Pollastri S, Olivi L, Huang Q Z, Liu H, Sanson A, Sun Q, Liang E J, Xing X R and Chen J 2020 *Scripta. Mater.* **187** 119
[16] Heinen J, Ready A D, Bennett T D, Dubbeldam D, Friddle R W and Burtch N C 2018 *ACS. Appl. Mater. Inter.* **10** 21079
[17] Schneider C, Bodesheim D, Ehrenreich M G, Crocellà V, Mink J, Fischer R A, Butler K T and Kieslich G 2019 *J. Am. Chem. Soc.* **141** 10504
[18] Wang C, Chu L H, Yao Q R, Sun Y, Wu M M, Ding L, Jun Y, Na Y Y, Tang W H, Li G N, Huang Q Z and Lynn J W 2012 *Phys. Rev. B* **85** 220103
[19] Takenaka K and Takagi H 2005 *Appl. Phys. Lett.* **87** 261902
[20] Hester B R, Hancock J C, Lapidus S H and Wilkinson A P 2016 *Chem. Mater.* **27**
[21] Han F, Hu L, Liu Z, Li Q, Wang T, Ren Y, Deng J X, Chen J and Xing X 2017 *Inorg. Chem. Front.* **4** 343
[22] Hester B R and Wilkinson A P 2018 *Inorg. Chem.* **57** 11275
[23] Morelock C R, Gallington L C and Wilkinson A P 2015 *J. Solid. State. Chem.* **222** 96
[24] Morelock C R, Gallington L C and Wilkinson A P 2014 *Chem. Mater.* **26** 1936
[25] Hu L, Chen J, Fan L L, Ren Y, Rong Y C, Pan Z, Deng J X, Yu R B and Xing X R 2014 *J. Am. Chem. Soc.* **136** 13566
[26] Chen J, Gao Q L, Sanson A, Jiang X X, Huang Q Z, Carnera A, Rodriguez C G, Olivi L, Wang L, Hu L, Lin K, Ren Y, Lin Z S, Wang C, Gu L, Deng J X, Attfield J P and Xing X R 2017 *Nat. Commun.* **8** 14441
[27] Yang C, Zhang Y G, Bai J M, Qu B Y, Tong P, Wang M, Lin J C, Zhang R R, Tong H Y, Wu Y, Song W H and Sun Y P 2018 *J. Mater. Chem. C* **6** 5148
[28] Baxter S J, Hester B R, Wright B R and Wilkinson A P 2019 *Chem. Mater.* **31** 3440
[29] Brink F J, Withers R L and Norén L 2002 *J. Solid. State. Chem.* **166** 73
[30] Yang B, Wang J, Liu X and Zhao M 2018 *Phys. Chem. Chem. Phys.* **20** 4781
[31] Cao W, Huang Q, Rong Y, Wang Y, Deng J, Chen J and Xing X 2016 *Inorg. Chem. Front.* **3** 856
[32] Wang J P, Chen Q D, Li S L, Ji Y J, Mu W Y, Feng W W, Zeng G J, Liu Y W and Liang E J 2018 *Chin. Phys. B* **27** 066501
[33] Li Y, Gao Q L, Chang D H, Sun P J, Liu J Z, Jia Y, Liang E J and Sun Q 2020 *J. Phys. Condens. Mater.* **32** 455703
[34] Kresse G and Furthmuüller J 1996 *Phys. Rev. B* **54** 11169
[35] Kresse G and Joubert D 1999 *Phys. Rev. B* **59** 1758
[36] Perdew J P, Burke K and Ernzerhof M 1996 *Phys. Rev. Lett.* **77** 3865
[37] Togo A, Oba F and Tanaka I 2008 *Phys. Rev. B* **78** 134106
[38] Wang L, Yuan P F, Wang F, Sun Q, Guo Z X, Liang E J and Jia Y 2014 *Mater. Chem. Phys.* **148** 214
[39] Wang Z, Wang F, Wang L, Jia, Y and Sun Q 2013 *J. Appl. Phys.* **114** 063508
[40] Chang D H, Liu Y M, Rao F F, Wang F, Sun Q and Jia Y 2016 *Phys. Chem. Chem. Phys.* **18** 14503
[41] Wang C Y, Chang D H, Gao Q L, Liu C Y, Wang Q G, Huang X W and Jia Y 2020 *Phys. Chem. Chem. Phys.* **22** 18655
[42] Ehrlich V P, Plöger F and Pietzka G 1955 *Z. Anorg. Allg. Chem.* **282** 19
[43] Miller W, Mackenzie D S and Evans K E 2009 *J. Mater. Sci.* **44** 5441
[44] Li C W, Tang X, Muñoz J A, Keith J B, Tracy S J, Abernathy D L and Fultz B 2011 *Phys. Rev. Lett.* **107** 195504
[45] Gao Q L, Wang J Q, Sanson A, Sun Q, Liang E J, Xing X R and Chen J 2020 *J. Am. Chem. Soc.* **142** 6935
[46] Gao Q L, Shi X W, Venier A, Carnera A, Huang Q Z, Wu H, Chen J, Sanson A and Liang E J 2020 *Inorg. Chem.* **59** 14852
[47] Liu Y M, Wang Z H, Wu M Y, Sun Q, Chao M J and Jia Y 2015 *Comp. Mater. Sci.* **107** 157